

# Shape, motion and deformation analysis of 2D echocardiographic sequences.

## Examples of application to the characterization of myocardial (dys)function

Glòria Macià Muñoz, Biomedical engineering, UPF, Barcelona, [gloriamaciamunoz@gmail.com](mailto:gloriamaciamunoz@gmail.com)

### Abstract

*During the last years, there have been large advances on the understanding of cardiac mechanics, and in particular shape, motion and deformation. However, it is important to comprehend how these features interrelate and how they can be interpreted to refine the clinical diagnosis. The goal of this article is to illustrate the use of 2D ultrasound (US) cardiac motion sequences on some typical cardiac pathologies. Thus, a computer program has been written in MATLAB language, which allows the user to easily obtain and visualize information about myocardial shape, motion (displacement and velocity) and deformation (strain) along the left ventricle (LV) myocardium wall during the cardiac cycle.*

*The method is applied to pre-processed data from 2D US sequences of four different subjects: two healthy volunteers, one patient with left ventricular mechanical dyssynchrony from left-bundle-branch-block, and one patient with hypertrophic cardiomyopathy. The interpretation based on these features was corroborated with other analyzing techniques such as electrocardiogram (ECG) and visual interpretation by experienced clinical observers.*

### 1. Introduction

During the last years, there have been large advances on the understanding of cardiac function, including shape, motion and deformation. However, the clinical applicability of myocardial motion and deformation comparison techniques remains limited: most of the studies just carry out simplistic measurements of e.g. dyssynchrony (peak values or timing measurements) or other clinical and image-based parameters, which turned out to be as promising and advertised as misleading. [1]. On the other hand, there is a much smaller number of studies which carry on a complete analysis: at a clinical level sometimes this degree of detail may not be necessary and, at a technical one, the interrelation of different features involves some difficulty.

Furthermore, more classical measurements performed in daily clinical routine, such as electrocardiogram (ECG) and visual interpretation of the cardiac pump function present the inconvenient of being extremely determined by the way they were carried out. This specificity not only makes harder to get a second medical opinion but also interferes with the personal health record (PHR) initiative. The PHR initiative stands in contrast to the more widely used electronic medical record, which is operated by institutions and contains data entered by clinicians or also billing data to support insurance claims[2].

The objective of this scientific article is to illustrate the use of a practical tool to analyze 2D ultrasound (US) cardiac motion sequences, which may allow the

user to obtain in a easy and quick way information about position (shape and displacement), velocity and strain along the myocardium wall during the cardiac cycle and to understand how these parameters are interrelated. Therefore a computer program has been written in *MATLAB*, a high-performance language for technical computing. It integrates computation, visualization, and programming in an easy-to-use environment where problems and solutions are expressed in mathematical notation. [3] In addition, the results are contrasted with the ECG and visual interpretation of the sequences to see whereas or not the same conclusion can be reached and, if possible, which additional information the software can supply.

### 2. Objectives

For this purpose, several scientific articles that exhibit the potential of recent techniques for extracting image data information have been reviewed. These studies were used as a starting point to establish which issues were important to address when assessing cardiac function, how regional deformation and myocardium contractibility are related [4] and how noninvasive clinical tools combined with knowledge of heart mechanics and physiology enables to interpret alterations in myocardial deformation and to extract clinically relevant conclusions [5]. For instance, in the case of cardiac pathologies such as hypertrophic cardiomyopathy, US deformation imaging, either by Doppler myocardial imaging or speckle tracking, turned out to be more sensitive than standard echocardiography, allowing the detection, identification and corresponding treatment of myocardial dysfunction at an early stage, which is of high clinical importance [6].

Finally, these new software techniques are also useful in understanding therapy outcome since they allow clinicians to visualize, in a integrated way, different cardiac features (shape, motion and deformation). With regard to left ventricular (LV) dyssynchrony (DYS), for example, septal deformation can be used to infer integrated information on dyssynchrony and regional contractility, and thereby may help in understanding cardiac resynchronization therapy outcome [7].

### 3. Methods

#### 3.1 Data exportation and pre-processing

The data used in this article comes from 2D ultrasound (US) sequences (4-chamber view) of four different volunteers, using the framework adapted from [8]. The myocardial wall has been automatically tracked along the 2D-US sequences using a speckle tracking algorithm from commercial software (Echopac software v.110.1.2, GE Healthcare, Milwaukee, WI, USA). It propagates a segmentation of the myocardium along the whole sequence and allows exporting the Cartesian coordinates of each point of the myocardial wall over the cardiac cycle. Drift correction was applied in order to make positions at the beginning and end of the cardiac cycle coincide.

The data were temporally aligned based on the timing of the following physiological events: the onset of the QRS complex, which determines the cycle start and end.

The processed data included 4 patients from *Hospital Clínic de Barcelona*: 2 healthy volunteers, 1 patient with left-ventricular dyssynchrony (left-bundle-branch-block) and 1 patient with hypertrophic cardiomyopathy. The study complied with the declaration of Helsinki was approved by the Local Ethics Committee, and informed consent was

obtained from each participant.

These pre-processing steps were already provided as part of the engineering lab this work is based upon. This work focuses on the analysis of these data.

#### 3.2 Data visualization

It is relevant to mention that, after the calculation of the different parameters for the characterization of myocardial (dys)function as explained in the subsequently sections, they have been visualized in three different ways: *imagesc* MATLAB function, *plotshaded* function and *surf* function (**Figure 1**) In this section, we discuss the relevance of each of these representations to visualize our data.

In the first case, the value of the feature is plotted, separately, for each point, frame time and subject. *Imagesc* function scales a matrix data to the full range of the current colormap and displays the image (e.g *imagesc(C)* displays C as an image). In our case, the columns of the matrix will represent the variable “frame time” and rows “point”. Notice that *imagesc* function will be the most used type of visualization in the article due to its precision in data representation.

The second way of representation is using *surf* function: *surf(Z)* creates a 3D shaded surface from the z components in matrix Z. Z specifies the color data, as well as surface height, so color is proportional to surface height. Nevertheless, when there are no clear peaks in the represented feature and the amount of points is big (i.e velocity is being plotted for 83 time frames at each of the points) *surf* function turns out to be confusing.

In the third case, on the contrary, the information of the data points is classified into lateral or septal according to their position respect to the apex (the point of maximum height in the LV). Next, the maximum and the minimum of the feature of study (e.g position, displacement, velocity) in each region (septal or lateral) are represented enclosing a color shaded region on which the expected value of the

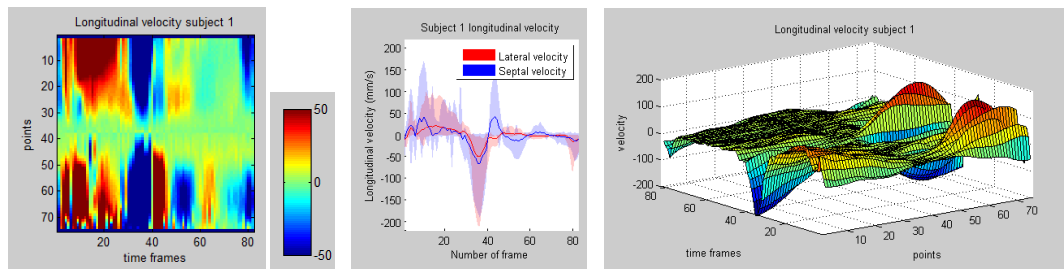


**Figure 1:** Example of the three methodologies of visualization used for longitudinal velocity of subject 1 (from left to right: *imagesc*, *plotshaded* and *surf* function). Notice that “End-Systole” occurs always at time frame 27, “End-Diastole” at  $t = 83$  and the position of the apex varies among subjects (in subject 1 is placed at point = 40). Therefore, points from 0 to 40 correspond to the septal wall and from 40 to 74 to the lateral one.

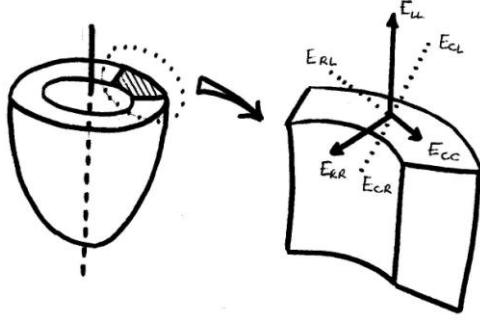


**Figure 2:** Schematic diagram demonstrating the three dimensional circumferential - radial - longitudinal (RCL) coordinate system used for strain calculation.

feature in this region is drawn. This sort of representation has the advantage of simplifying the complexity of the system in one shaded region (compressed between the maximum and the minimum values for the feature) and a curve showing the general behavior. However, in comparison with the *imagesc* function, it is not so informative: this simplified representation also hides some valuable information.

### 3.3 Local system of coordinates: longitudinal and radial directions at each point of the myocardium

Due to the 3D cardiac geometry and the complex fibers disposition, myocardial features can be represented by two different coordinate systems: the radial-fiber-crossfiber coordinate system, which is based on the fiber direction within the myocardial tissue; the radial-circumferential-longitudinal (RCL) coordinate system (**Figure 2**). The RCL coordinate system is based on the cardiac geometry and, thus, is more convenient to handle in clinical practice [9].

The longitudinal direction at each point of the myocardium and at each instant of the cycle is computed using a centered scheme:

$$\Delta_{long}(x_i, t_j) = \frac{\varphi(x_{i+1}, t_j) - \varphi(x_{i-1}, t_j)}{2}$$

and

$$e_{long} = \frac{\Delta_{long}}{|\Delta_{long}|} \text{ if } i < \frac{\text{number of points}}{2}$$

$$e_{long} = -\frac{\Delta_{long}}{|\Delta_{long}|} \text{ if } i \geq \frac{\text{number of points}}{2}$$

The radial direction  $e_{radial}$  corresponds to the longitudinal rotated by 90 degrees:

$$e_{radial} = \begin{bmatrix} 0 & -1 \\ 1 & 0 \end{bmatrix} \times e_{long}$$

The output of these computations is illustrated on subject 1 at end-diastole (**Figure 3**).

### 3.4 Cardiac shape

#### 3.4.1 Myocardial shape at the beginning of the cycle, at end-systole and end-diastole

The process described above returns as an output a matrix of type cell containing 4 elements, each element being a different subject. In addition, each subject contains two components of position  $\varphi = [\varphi_x, \varphi_y]$ , which are 2D objects with dimensions: number of frames in the cycle  $\times$  number of points along the myocardium. The notation used in this section is ' $t_j$ ' for each instant of the cycle (corresponding to a frame number) and ' $x_i$ ' for each point of the myocardium wall. Notice that, although all subjects have 83 frames (because data has been previously temporally aligned, as described in Section 3.1), they have different number of points along the myocardium.

In this section, the myocardial shape at the beginning of the cycle (frame number = 1) at end-systole (frame number = 27) and end-diastole (frame number = 83)

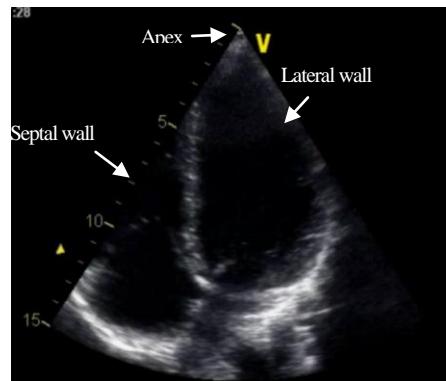
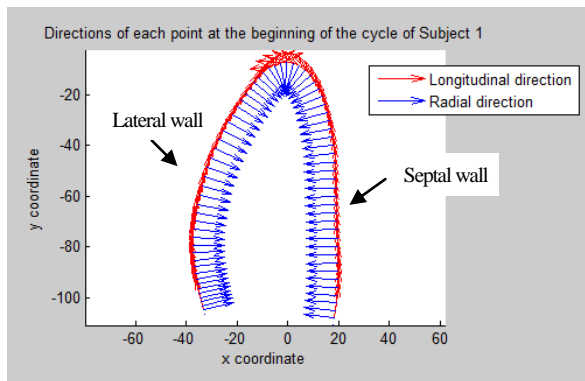


**Figure 3:** On the left, longitudinal and radial direction of subject 1 at each point of the myocardium. On the right, the real 2D ultrasound (US) sequences. Apex, septal and lateral walls are indicated in the figures.

is plotted in the same figure using *subplot* function in order to visualize and contrast the data of each patient.

### 3.4.2 Length of the entire myocardial shape at end-systole ( $L_{ES}$ ), end-diastole ( $L_{ED}$ ) and ratio

In order to compute the total length of the entire myocardial shape at a concrete instant of time, which could be either end-systole or end-diastole, the following procedure schematized in **Figure 4** has been used:

$$\Delta long_{x(j=83,i)} = \frac{\varphi_{x(j=83,i+1)} - \varphi_{x(j=83,i-1)}}{2}$$

$$\Delta long_{y(j=83,i)} = \frac{\varphi_{y(j=83,i+1)} - \varphi_{y(j=83,i-1)}}{2}$$

$$|\Delta long_{(j=83,i)}| = \sqrt{\Delta long_x^2 + \Delta long_y^2}$$

$$L_{ED} = \sum_{i=1}^{No.points} |\Delta long_{(j=83,i)}|$$

where  $\Delta long_{x \text{ or } y(j,i)}$  is the difference in position between two adjacent points in the horizontal or vertical direction and  $\Delta long_{(j,i)}$  corresponds to the norm of both components. Finally,  $L_{ED}$  is defined as the total length of the myocardial shape of at a certain instant of time ( $t = j$ ) and it is calculated as the sum of the norms over all the points at the same instant of time (time frame = 83 = *endDiastole*). The same procedure is repeated for the rest of the subjects at the *endDiastole* and *endSystole* frames. To conclude, the relative difference between the maximum length (*endDiastole*) and the minimum one (*endSystole*) for each subject has been computed as  $\frac{L_{ED} - L_{ES}}{L_{ED}}$ . The ratio of LV lengths is an analogy to the ejection

fraction  $E_f = \frac{V_{ED} - V_{ES}}{V_{ED}} \times 100$ , commonly used in clinical practice to interpret the ventricle performance (i.e blood ejection).

### 3.5 Cardiac motion: displacement and velocities

#### 3.5.1 Radial and longitudinal displacement

The displacement in Cartesian coordinates at each point  $x_i$  and time  $t_j$  is calculated as the difference in position between times  $t_j$  and  $t_0$ :

$$\begin{bmatrix} u_x(x_i, t_j) \\ u_y(x_i, t_j) \end{bmatrix} = \begin{bmatrix} \varphi_x(x_i, t_j) - \varphi_x(x_i, t_0) \\ \varphi_y(x_i, t_j) - \varphi_y(x_i, t_0) \end{bmatrix}$$

Then, its radial and longitudinal components are computed as follows:

$$\begin{bmatrix} u_r \\ u_l \end{bmatrix} = P^{-1} \begin{bmatrix} u_x \\ u_y \end{bmatrix} \text{ where } P = \begin{bmatrix} e_{radial,x} & e_{long,x} \\ e_{radial,y} & e_{long,y} \end{bmatrix}$$

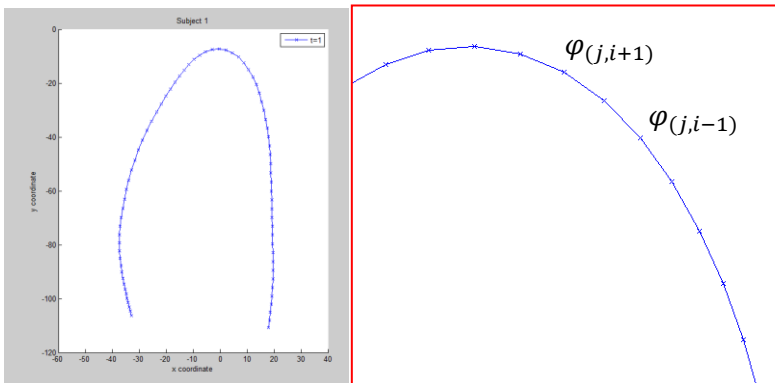


**Figure 4:** Illustration of the computation of the length of the entire myocardial centerline.

### 3.5.2 Radial and longitudinal velocity

Myocardial velocities are obtained from the temporal derivative of displacements:

$$\begin{bmatrix} v_r \\ v_l \end{bmatrix} = \begin{bmatrix} \frac{d(u_r)}{dt} \\ \frac{d(u_l)}{dt} \end{bmatrix}$$

which has been calculated as follows:

$$\begin{bmatrix} v_{r(x_i, t_j)} \\ v_{l(x_i, t_j)} \end{bmatrix} = \begin{bmatrix} \frac{u_r(x_i, t_j) - u_r(x_i, t_{j-1})}{time\_interval} \\ \frac{u_l(x_i, t_j) - u_l(x_i, t_{j-1})}{time\_interval} \end{bmatrix}$$

where *time\_interval* corresponds to the period of framing (*time\_interval* = 0.01 s).

Afterward, radial and longitudinal velocities spatiotemporal information is visualized in three different ways: using first *imagesc* MATLAB function, *plotshaded* function and *surf* function.

### 3.6 Cardiac deformation: longitudinal strain

In this section, cardiac deformation will be computed. Deformation is generally defined as an alteration of shape, as by pressure or stress. In this concrete case, cardiac deformation is caused by the pressure (exerted by the wall stress), the strength of the neighboring areas of the wall and, principally, the active contraction of the heart muscle [4] (**Figure 5**). Nonetheless, this article will focus in strain, which is of great relevance in the medical field since it has a close relationship with heart contractibility.

Although there exist several ways to compute strain, for this particular case of large deformations,

Lagrangian strain has been chosen under the assumption that the deformation between two instants of time is large (since it is the accumulation of little deformations between consecutive frames) and calculated as follows:

$$\frac{|\Delta_{long}(x_i, t_j)| - |\Delta_{long}(x_i, t_0)|}{|\Delta_{long}(x_i, t_0)|}$$

Observe that the formula corresponds to a relative change of the original lengths, and more precisely, to how an element defined by a longitudinal neighborhood elongates in the longitudinal direction. Therefore, it corresponds to the component  $E_{l,1}$  of the strain tensor  $E_{RCL} = \begin{bmatrix} E_{r,r} & E_{r,l} \\ E_{l,r} & E_{l,l} \end{bmatrix}$ . Unfortunately, the same could not be done in the radial direction, since there is no radial neighborhood defined in the data exported from the speckle tracking software.

Finally, consider that due to the 3D cardiac geometry myocardial strain is represented by the radial-circumferential-longitudinal (RCL) coordinate system (Figure 1 section “3.3 Local system of coordinates”). In the later, circumferential strain ( $E_{c,c}$ ) describes circumferential shortening in the short axis plane in a direction tangential to the epicardial surface; radial strain ( $E_{r,r}$ ) describes myocardial thickening in a radial direction towards the center of the ventricle; and, longitudinal strain ( $E_{l,l}$ ) represents base to apical shortening along the ventricular long axis. Therefore, the data matrix should be  $3 \times 3$  but, since we have worked with 2D data it is  $2 \times 2$ .

Passive loading	Active contractile force	Tissue elasticity	Total regional deformation
<ul style="list-style-type: none"> <li>• cavity pressure</li> <li>• geometry</li> <li>• neighbouring segment interaction</li> </ul>	<ul style="list-style-type: none"> <li>• activation</li> <li>• electro-mechanical coupling</li> <li>• perfusion</li> </ul>	<ul style="list-style-type: none"> <li>• fibre structure</li> <li>• fibrosis</li> </ul>	<ul style="list-style-type: none"> <li>• strain</li> </ul>

$$WallStress_{passive}(t) - ContractileForce_{active}(t) = Elasticity \times Deformation(t)$$

**Figure 5:** Relationship between local forces and deformation. Picture adapted from [4].



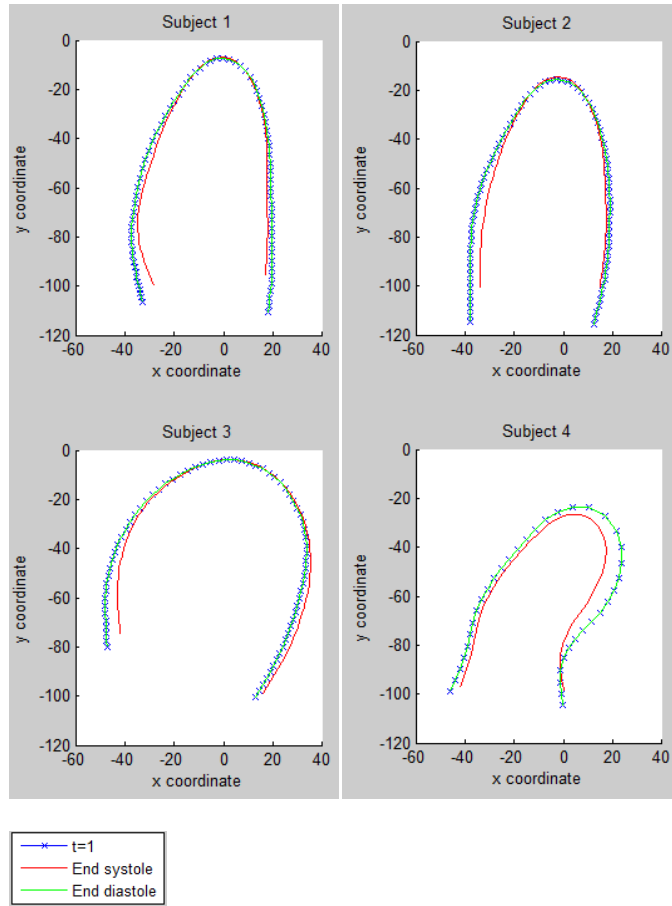


**Figure 6:** Myocardial shape at the beginning of the cycle, at end-systole and end-diastole for each of the subjects.

## 4. Results

### 4.1 Local system of coordinates: longitudinal and radial directions at each point of the myocardium

**Figure 2** shows both radial and longitudinal directions at every location along the myocardium. On the one hand, notice that the radial direction points to the center of the cavity, so it provides valuable information about the relative motion of each point respect to the center of the LV cavity. On the other hand, due to our convention, longitudinal direction is tangent to every point.

### 4.2 Cardiac shape

#### 4.2.1 Myocardial shape at the beginning of the cycle, at end-systole and end-diastole

Myocardial shape is used to compare the different subjects at concrete time frames of the cardiac cycle.

**Figure 6** represents the shape of the LV at the beginning of the cycle, at the end of the systole and at the end of the diastole for the four subjects. Observe that in all the cases, the LV at the end of the systole is smaller than at the beginning of the cycle (as should be expected since the end of the systole is the moment of maximum heart contraction). Furthermore, notice how in the end of the diastole, which is the final of the cycle, the shape coincides with the one at  $t = 1$ , also logical since cardiac contraction is a cyclic process.

However, subjects 1 and 2 have a fairly regular shape in comparison to subject 3 that has a dilated cavity, and subject 4 that seems to have a smaller and unusual shape. This information indicates that subjects 1 and 2 are probably healthy, whereas 3 and 4 are most likely pathological. No further interpretations can be given at this stage, as such data do not include LV dynamics. These aspects will be studied in the next sections.

#### 4.2.2 Length of the entire myocardial shape at end-systole ( $L_{ES}$ ), end-diastole ( $L_{ED}$ ) and ratio

The ratio of LV lengths is an indirect measurement of

	$L_{ED}$ (mm)	$L_{ES}$ (mm)	Ratio (%)
Subject 1	221.441	198.368	0.104
Subject 2	218.212	188.193	0.138
Subject 3	216.531	208.605	0.037
Subject 4	189.043	167.113	0.116

**Table 1:** Length of the entire myocardial shape at end-systole ( $L_{ES}$ ), end-diastole ( $L_{ED}$ ) and ratio for each of the subjects.

the ejection fraction in order to interpret the ventricle performance (i.e blood ejection).

The data of **Table 1** show that in all the cases, the length of the LV at the beginning of the cycle is bigger than the one at the end of the systole, not surprising since it is the moment of maximum contraction.

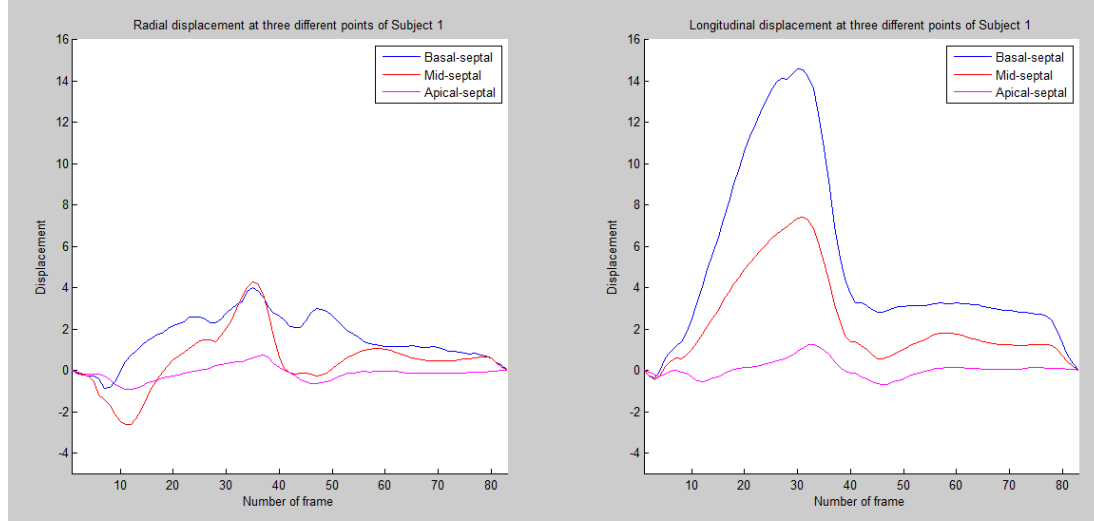


**Figure 7:** Radial and longitudinal displacement data (mm) along the whole cycle for subject 1 at basal-septal, mid-septal and apical-septal locations.

It is interesting to notice that the shortening ratio of subject 3 is significantly smaller than the rest. In the previous section it has already pointed out that this subject is probably pathological. This pathology may difficult blood ejection and, as a consequence, the shortening ratio is diminished. Subject 4 has a ratio comparable to the ones of subjects 1 and 2 but shorter lengths and therefore could correspond to either a shorter or lighter individual or to a pathological case.

Finally, it is important to take into account that, although in this section the ratio of LV lengths was used, the ejection fraction  $E_f = \frac{V_{ED} - V_{ES}}{V_{ED}} \times 100$ , commonly used in clinical practice, would have been

a more accurate measure to understand the ventricle performance, since it works with volumes not lengths. A normal ejection fraction is around 55% [10], which means that at the end of the contraction process, the volume of the LV has approximately been reduced by half. This is the value we would expect to find in subjects 1 and 2, whereas subjects 3 and 4 would have smaller values.

### 4.3 Radial and longitudinal displacement

Radial and longitudinal displacements are computed for each of the subjects at different levels to see if cardiac motion is normal.

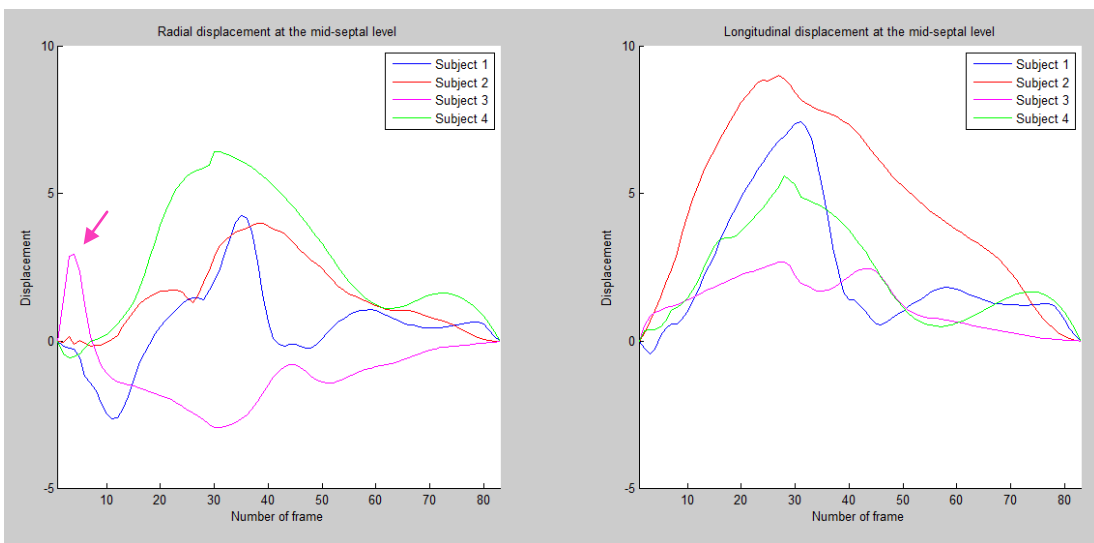


**Figure 8:** Radial and longitudinal displacement data (mm) along the whole cycle for each of the subjects at mid-septal level. Observe that subject 3 has little displacement, with an abnormal motion in the radial direction the beginning of the cycle: septal flash (arrow), as described in Parsai et al. [12]

In this section, the displacement data is first visualized along the whole cycle for subject 1 at basal-septal, mid-septal and apical-septal locations, respectively (**Figure 7**). Observe that there is less displacement (more visible in the longitudinal direction) as it approaches the apex. Also see the characteristic motion pattern of a healthy subject, with marked contraction and subsequent relaxation phases.

The displacement data have been compared between all the subjects at the mid-septal level (**Figure 8**). Notice that both subjects 1 and 2 (identified before as healthy individuals) have a clear pattern of contraction and relaxation, although this pattern is much more marked in the subject 1. Even though both have normal patterns, subject 1 has a rapid relaxation phase (quick diastole), whereas subject 2 has a much slower relaxation, probably because of its age (alterations of normal cardiac function may occur with aging) [11]. Then, subject 3 has little displacement, with an abnormal motion in the radial direction at the beginning of the cycle: septal flash (marked in **Figure 8**), a rather prevalent pattern for individuals suffering from this type of left ventricular dyssynchrony (left-bundle-branch-block, further details in [12]). Finally, subject 4 appears to have a relatively normal motion, although it is a pathological case. Deformation analysis (strain pattern) may help in providing additional information.

However, last figures only provided information about one point (mid-septal level) or three different points (basal-septal, mid-septal and apical-septal

locations) but one patient (subject 1). For a more precise visualization of the results, *imagesc* function should be used, which allows us to plot radial and longitudinal displacement at each of the points for every time frame in all four subjects.

Regarding the displacement, in **Figure 9** it is more pronounced in the basal-septal level and it decreases gradually (basal-septal, mid-septal , apical-septal ) until it reaches a minimum at the apex, which corroborates the observations of Figure 7. Moreover, taking the apex as the axis of symmetry, it can be seen that the contraction is synchronous (i.e septum and lateral walls contract coordinated) in all cases except in subject 3, a case of dyssynchrony and, thus, altered patterns of movement. Besides, subject 3 radial velocity map presents a reddish spot in the beginning of systole at the septum wall. This mark, known as septal flash, corresponds to an anomalous septal movement, characteristic of subjects with this type of dyssynchrony that can be seen in the video attached as supplementary material.

To conclude, we observe on the longitudinal displacement data a clear contraction of the walls during systole (positive values on the map) and a subsequent relaxation. Regarding the radial displacement, it can be seen how left ventricle goes to the inside of the cavity during systole (positive values) and returns to its resting shape in diastole (as expected).

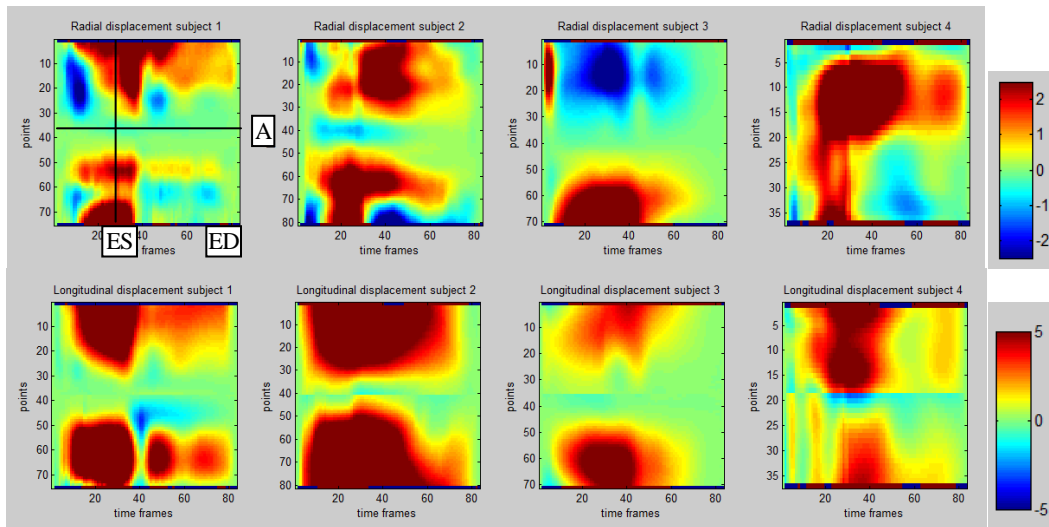


**Figure 9:** Spatiotemporal representation of radial and longitudinal displacement for each of the subjects using *imagesc* function. “ES” corresponds to “End-Systole” always at time frame 27, “ED” corresponds to “End-Diastole” at  $t = 83$  and “A” corresponds to “apex” (lowest superficial part of the heart).



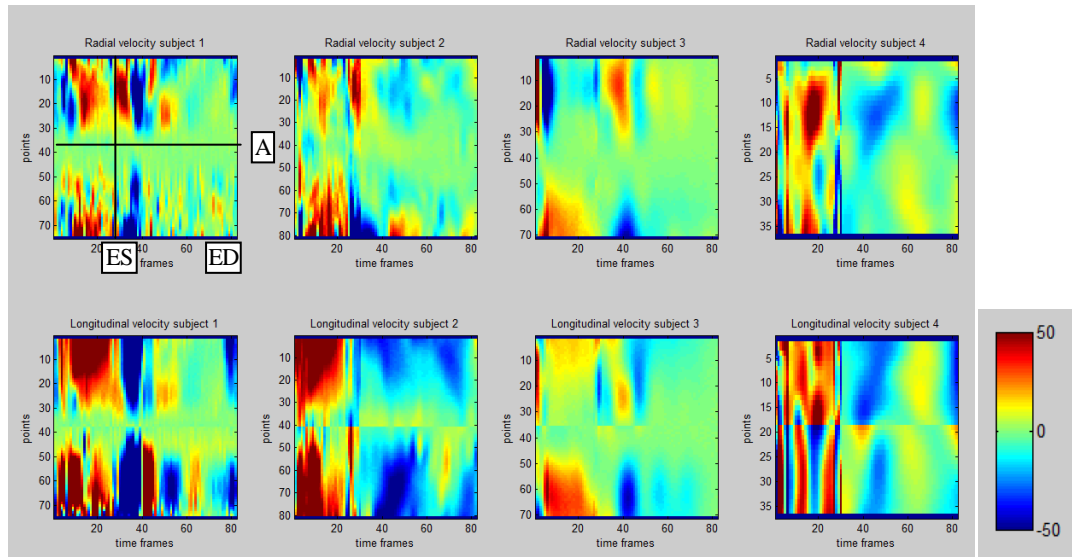


**Figure 10:** Spatiotemporal representation of radial and longitudinal velocity for each of the subjects using *imagesc* function. “ES” corresponds to “End-Systole” always at time frame 27, “ED” corresponds to “End-Diastole” at  $t = 83$  and “A” corresponds to “apex” (lowest superficial part of the heart).

#### 4.4 Radial and longitudinal velocity

As radial and longitudinal displacements, both types of velocities are computed for each of the subjects at different levels to see if cardiac motion is normal.

In **Figure 10**, the value of both types of velocities is plotted, separately, for each point (vertical axis), frame time (horizontal axis) and subject (using *subplot MATLAB* function). To understand the maps, it is necessary to have a deep comprehension of the existing relation between velocity and displacement. Velocity is calculated as the derivative of the displacement, given that this one is infinitesimal. As a consequence, it is not of surprising that both features present a very similar behavior. As can be seen in **Figure 11**, where both maps are compared, velocity map is the derivative of the displacement map respect to the horizontal dimension (time frames). Therefore, if displacement increases, velocity is positive (reddish colors); velocity is negative (bluish colors) if it decreases. When displacement is constant, velocity is nil.

As it happened with the displacement, the velocity maps present symmetry respect to the apex (i.e. synchronous contraction) except in case of the subject 3, in whose graph of radial velocity can also be appreciated the septal flash. As observed in section « 4.3 Radial and longitudinal displacement », subject 3 has nearly null velocity, with an abnormal motion in the radial direction at the beginning of the cycle (early activation of the septum), which corresponds to a

classical pattern for individuals suffering from left ventricular dyssynchrony [12].

On the one hand, observe that subjects 1, 2 and even 4 present a similar pattern: positive longitudinal and radial velocities (i.e. reddish) all through the contraction phase, which corresponds to frame times [1-27], and negative values (i.e. bluish) afterwards, during the relaxation phase. Nevertheless, subject 3 appears to have a much difficult to discern systole and diastole. On the other hand, all subjects present small velocities (represented by light colors) in points close to the apex, since displacement is approximately constant in these points whereas in the regions nearby to the mitral valve, velocity turns to be higher (also logical considering that in the systolic process, contraction starts in the apex, propagates throughout the myofibers and finishes in a coordinate way on the basal level of the ventricles, where it should have generated enough force to overcome

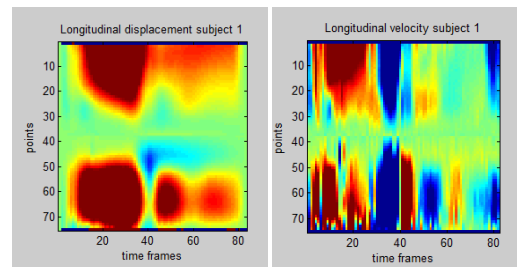


**Figure 11:** Longitudinal displacement and velocity of subject one displayed using *imagesc* function. Since velocity map is the derivative of the displacement map respect to the horizontal dimension (time frames) when displacement increases, velocity is positive and velocity is negative if it decreases. If displacement is constant, velocity is zero.

aorta pressure (normally around 120 mmHg).

Notice also that, due to the relationship previously mentioned between both magnitudes, when the displacement increases, the velocity map shows positive values whereas, if it decreases, these are negative. Finally, the transition between the septal and lateral walls of the myocardium is much easier to see than in the maps of displacement because of the sudden change of sign of direction vectors defined in paragraph “3.3 Local system of coordinates: longitudinal and radial directions at each point of the myocardium”.

#### 4.5 Cardiac deformation: longitudinal strain

Longitudinal strain along the myocardium has been computed for each of the subjects in order to contrast the information provided by the motion analysis.

The strain along the whole cardiac cycle at mid-septal level has been represented in **Figure 12**. Note that strain is a normalized magnitude and, consequently, it is dimensionless (or expressed in %).

If the strain between the four subjects is compared, the following observation can be made: the strain is negative, corresponding to the contraction phase;

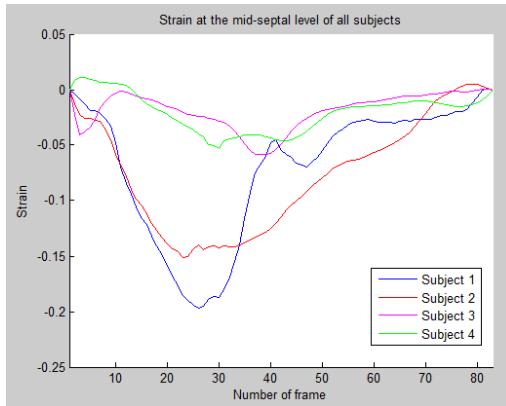


**Figure 12:** Strain for each of the subjects during the whole cardiac cycle at mid-septal level.

subjects 1 and 2 have a normal strain pattern, even

though again a quick relaxation is seen in subject 1 and a much slower for subject 2; subject 3, who had an anomalous displacement also has an anomalous strain. Therefore, it is corroborated as the case of dyssynchrony. Lastly subject 4, which had a normal pattern of displacement, has a practically zero strain. Consequently, this points out in the direction of local damage of the myocardium (and therefore, in our case, the patient with hypertrophy), since it has little local contraction due to the fibers damage in the hypertrophic region (refer to the US videos for further justifications). This argument also reinforces the observations about the LV shape seen in section 4.2.2, in which subject 4 presented less volume inside the cavity due to the hypertrophy.

In **Figure 13**, be aware that in case of subjects 1 and 2 (healthy individuals), the strain presents a symmetrical pattern (synchronous contraction), excluding a small data artifact in subject 1, a noise that might come from the proximity of the points to the mitral valve.

In case of subject 3, a normal pattern is seen in the lateral wall but it presents very little contraction in the septum, which confirms the suspected pathology. Finally, the hypertrophic patient shows little contraction due to the pathological thickening of its myocardium, except in the apex, where the wall thickness is normal and so is the strain.

#### 4.6 Clinical experts US sequences interpretations

The interpretation based on the features (motion and deformation) was corroborated with other analysis techniques such as electrocardiogram (ECG) and visual interpretation by experienced clinical observers.

The two doctors have interpreted the video of the healthy subjects (patients 1 and 2), since it was a US 2D sequence of suitable duration, good quality of image (even the coronary vein can be intuited) and

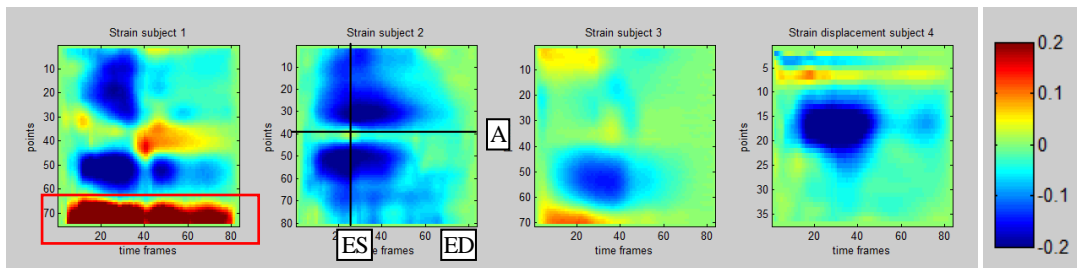


**Figure 13:** Spatiotemporal representation of strain for each of the subjects using *imagesc* function. Marked in red, a little artifact of the data (probably caused by the mitral valve influence on the speckle tracking accuracy).

obtained in different planes. Both experts have coincided that: the images and the ECG seemed to be normal and they observed neither indications of thrombi nor any other evident pathology. Nevertheless, one of the doctors stated that the right atrium was a little bit bigger than the left one (when normally is the other way around), which might be due to a bad position of the transducer (probably with something of tricuspid regurgitation).

In case of the subject 3, the doctors do not consider having sufficient information to interpret it adequately, since there is only a plane of short duration, although they point out a ventricular low mobility and increased atria. In fact, the left atrium is almost as big as the ventricle, probably due to a dysfunction of it, in spite of the fact that the contours of this one do not remain well delimited in the sequence. Another interesting fact is the mitral valve, very calcified and with a great quantity of echoes fluctuating. This may indicate that the density of the blood is high and therefore there exists an important probability of an embolism. The tricuspid valve also presents less movement than usually.

Finally, in reference to the subject 4, in spite of being a sequence of only one plane (apical) and short duration, both experts have affirmed that it is a case of hypertrophic cardiomyopathy. It can be clearly seen the thickness of the septum wall and the thickness of the auricles wall also lightly increased. Moreover, due to the thickness of the walls, the volume inside the heart cavities is reduced and small deformation can be appreciated in the sequences. Nevertheless the ultrasound scan is not ideal; there are many spontaneous echoes, so it would be adequate to lower the intensity of the transducer to obtain more contrast in the images.

## 5. Conclusions

The objective of this work was to illustrate the use of a practical tool to analyze data from 2D echocardiographic sequences. The overall objective was to comprehend the relations between myocardial shape, motion and deformation of the LV during the cardiac cycle, and interpret the meaning of these features with respect to our knowledge about some typical cardiac (ab)normal patterns. Observations were corroborated with simpler analysis techniques such as electrocardiogram (ECG) and visual interpretation from experienced clinical observers. We illustrated that our data representation may be

valuable tool for understanding cardiac function and refining clinical diagnosis.

The study of a few typical medical cases performed in this paperwork was just an example of the potential of the computational analysis of 2D echocardiographic sequences to the characterization of myocardial (dys)function. Therefore, for further works, it would be interesting to have a deeper understanding of the patterns, its variability within a healthy or unwell population and how they can evolve under treatment or due to certain pathology.

In addition, it may be of great usefulness to perform a detector of anomalies contrasting the different plots created by *imagesc* function, comparing the values of the healthy versus pathological subjects. For this purpose, it would be necessary to design an algorithm that normalizes the number of points of the subjects and allows the subtraction, point to point, of the features. Advanced statistical tools for analyzing populations may be also useful to reach a statistical definition of “normal” ranges.

Finally, it is important to mention that the methodology proposed in this research could be applied to other types of medical images; if 2D echocardiographic sequences have been chosen is because of their common use in their clinical routine, since 2D US image acquisition is cheaper than scanners or clinical resonance.

In any case, the computational analysis of 2D echocardiographic sequences is an approach of great interest that provides a vast quantity of information to the specialist, not only quantitative but also objective, which grants to this technique a promising future in the diagnostic field.

## 6. Acknowledgments

**This work has been done under the supervision of Nicolas Duchateau (Associate Professor at Universitat Pompeu Fabra). The author acknowledges Dr. Marta Sitges from Hospital Clínic, Barcelona for the access to the echocardiographic data and both, Dr. Antonio Martínez Rubio from Corporació sanitària Parc Taulí, Sabadell, and Dr. César Fernández del Prado from Hospital Sant Joan de Déu de Manresa, Althaia, for their expert clinical opinion.**

## 7. Bibliography

- [1] Fornwalt, B.K.: The dyssynchrony in predicting response to cardiac resynchronization therapy: A call for change. *Journal of the American Society of Echocardiography* 24, 180–184 (2011)
- [2] Personal health record:  
[http://en.wikipedia.org/wiki/Personal\\_health\\_record](http://en.wikipedia.org/wiki/Personal_health_record)
- [3] Matlab:  
<http://cimss.ssec.wisc.edu/wxwise/class/aos340/spr00/whatismatlab.htm>
- [4] Bijmens et al. Velocity and deformation imaging for the assessment of myocardial dysfunction. *Eur J Echocardiogr.* 2009; 10: 216–26
- [5] Bijmens et al. Myocardial motion and deformation: What does it tell us and how does it relate to function? *Fetal Diagn Ther.* 2012; 32: 5–16
- [6] Cikes et al. The role of echocardiographic deformation imaging in hypertrophic myopathies. *Nat Rev Cardiol.* 2010; 7: 384–96
- [7] Leenders GE et al. Septal deformation patterns delineate mechanical dyssynchrony and regional differences in contractility: analysis of patient data using a computer model. *Circ Heart Fail* 2012;5:87-96
- [8] Duchateau, N., De Craene, M., Pennec, X., Merino, B., Sitges, M., Bijmens, B.: Which Reorientation Framework for the Atlas-Based Comparison of Motion from Cardiac Image Sequences? *Lecture Notes in Computer Science* Volume 7570, 2012, pp 25-37 (2012)
- [9] Shehata *et al. Journal of Cardiovascular Magnetic Resonance* 2009 11:55  
doi:10.1186/1532-429X-11-55
- [10] Ejection fraction:  
<http://rehabilitateyourheart.wordpress.com/2013/03/19/do-you-know-your-hearts-ejection-fraction/>
- [11] Ji-zhu Xia, Ji-yi Xia, Gang Li, Wen-yan Ma and Qing-qing Wang; Left Ventricular Strain Examination of Different Aged Adults with 3D Speckle Tracking Echocardiography; 13 SEP 2013 | DOI: 10.1111/echo.12367
- [12] Parsai et al. Toward understanding response to cardiac resynchronization therapy: left ventricular dyssynchrony is only one of multiple mechanisms. *Eur Heart J* 2009; 30:940-949